

PAPER • OPEN ACCESS

Electrochromic and optical study of sol-gel TiO₂-MnO films

To cite this article: T Ivanova *et al* 2020 *J. Phys.: Conf. Ser.* **1492** 012028

View the [article online](#) for updates and enhancements.



IOP | ebooks™

Bringing together innovative digital publishing with leading authors from the global scientific community.

Start exploring the collection—download the first chapter of every title for free.

Electrochromic and optical study of sol-gel TiO₂-MnO films

T Ivanova^{1,4}, A Harizanova¹, T Koutzarova² and B Vetryuen³

¹Central Laboratory of Solar Energy and New Energy Sources,
Bulgarian Academy of Sciences, 72 Tzarigradsko Chaussee, 1784 Sofia, Bulgaria

²Acad. E. Djakov Institute of Electronics, Bulgarian Academy of Sciences,
72 Tzarigradsko Chaussee, 1784 Sofia, Bulgaria

³GREENMAT, Institute of Chemistry B6, University of Liege,
B6a Quartier Agora, 13 Allée du Six Août, 4000 Liège, Belgium

E-mail: tativan@phys.bas.bg

Abstract. We present a study on the structural, optical and electrochromic properties of sol-gel films of TiO₂ and TiO₂-MnO. The XRD analyses show that the incorporation of Mn in the TiO₂ host matrix inhibits the crystallization process, as compared to single TiO₂ films, which are well crystallized in anatase phase. This conclusion is supported by FTIR analysis. Adding Mn to the TiO₂ films leads to a significant narrowing of the optical band gap. The electrochromic characteristics of TiO₂-MnO films are better than those of the single titanium dioxide films after annealing at 300 °C.

1. Introduction

The electrochromic (EC) thin films are “smart” materials that change their optical properties under an applied small external voltage. EC layers and devices find practical applications in “smart” windows regulating the incoming/outgoing solar radiation in buildings [1], rear-view mirrors, information displays, thermal radiators etc. The transition metal oxides provoked the interest of researchers as EC materials due to their chemical stability, reversible color switching and good optical transparency. Another advantage is the possibility to enhance the EC properties by single or double doping or by forming composites [2]. The expected benefit is better color efficiency and durability, an extended switching potential range and improved reaction kinetics [3]. TiO₂ is studied due to its chemical, electrical and optical properties: high refractive index, small thermal expansion coefficient and transparency over a wide spectral range [4]. TiO₂ is an electrochromic cathodic material whose properties are strongly related to the method and conditions of deposition [5]. Manganese oxides have also generated considerable scientific and technological interest because of their electronic and magnetic properties [6]. Many attempts have been made to modify the physical, chemical and optical properties of TiO₂ by mixing with other oxides [7]. The TiO₂/MnO_x composites are studied for their improved optical and photocatalytic properties, and as a promising material for solar energy conversion [6, 8].

This paper describes the sol-gel deposition of TiO₂-MnO films and their structural, optical and electrochromic properties as depending on the annealing temperature.

⁴ To whom any correspondence should be addressed.



2. Experimental

The preparation of the sol solution for the deposition of TiO₂ films was reported previously [9]. The sol contained titanium ethoxide as a precursor and small amounts of glacial acetic acid and water. A certain amount of acetylacetone was used as a peptizing agent and stabilizer. The manganese precursor was Mn(NO₃)₃·4H₂O in the appropriate amount to obtain the TiO₂-0.25MnO system in molar parts. TiO₂ and TiO₂-MnO films were deposited by dip coating on glass, Si and conductive glass substrates. The preheating temperature was 300 °C/30 min. The coating and preheating procedures were repeated three times. The films obtained were annealed at 300 °C and 500 °C for one hour.

The XRD patterns were taken by a Bruker D8 XRD diffractometer using Cu K_α radiation ($\lambda_{K\alpha} = 1.54056 \text{ \AA}$) at a grazing incidence angle of 2° and a step time of 8 s. The FTIR measurements were conducted using a Shimadzu IRPrestige-21 FTIR spectrophotometer in the spectral range 350 – 4000 cm⁻¹. The optical measurements were carried out by a Shimadzu 3600 UV-VIS-NIR spectrophotometer.

The electrochromic behavior of the films was examined by cyclic voltammetry. The measurements were performed in a three-electrode cell with a Pt wire as a counter electrode and a saturated calomel electrode (SCE) as a reference electrode. The electrolyte was 1 M LiClO₄ in propylene carbonate (1 M LiClO₄+PC). The color change was detected by an attached optical system equipped with a chopped light source, a lock-in amplifier and a monochromator. The color efficiency (CE) qualifies the modulation of the optical properties of EC materials and is determined by the optical density ΔOD and the injected/ejected charge [10]. ΔOD is estimated from the transmittances in the bleached state and the colored state. CE is spectrally dependent, so that a comparison of the CE values is possible for a given wavelength only.

3. Results and discussions

The XRD patterns of the TiO₂ and TiO₂-0.25MnO films prepared on a Si substrate and treated at 500 °C/1hour are shown in figure 1.

The TiO₂ films annealed at 500 °C were fully crystallized with diffraction peaks consistent with the anatase phase (PDF 01-086-1157). The XRD study of the sol-gel TiO₂-MnO films treated at 500 °C revealed its lower crystallinity compared with single TiO₂ films obtained under the same technological conditions. Four lines indicated the anatase phase of TiO₂. The line at 44.6° was related to the Mn₂O₃ phase (JCPDS 41-1442) [11]; the very broad feature at 55.8° consisted of the overlapping contributions from anatase and MnO₂ phases (PDF - 00-012-0713). The results illustrate that the TiO₂-MnO was poorly crystallized and the MnOx fractions were almost amorphous. Adding Mn to the TiO₂ host inhibited the crystallization compared to the TiO₂ films (figure 1). Previous studies of sol-gel TiO₂-MnO powders [12] annealed at 560 °C/1 hour revealed the presence of rutile TiO₂, MnTiO₃ and MnTi₂O₄. In the case of thin films, the presence of rutile titania and mixed Ti-Mn oxide phases have not been detected either due to the XRD limit of detection or to the nano-crystallites being smaller than 5 nm [13].

We applied FTIR spectroscopy to complement the XRD analysis. The absorption above 1100 cm⁻¹ is usually related to organic residues (not shown). The FTIR spectra revealed bands around 3400 cm⁻¹ due to the OH stretching vibrations and the corresponding bending modes at 1600 cm⁻¹ [14] for TiO₂ and TiO₂-MnO. These bands vanished after the annealing at 500 °C. The presence of water could be related to adsorption of moisture from the environment or the sol-gel processing. The C-H bonds were observed at 2930 cm⁻¹ and 2855 cm⁻¹ [15]. The line at 2360 cm⁻¹ was assigned to C-O vibrations of

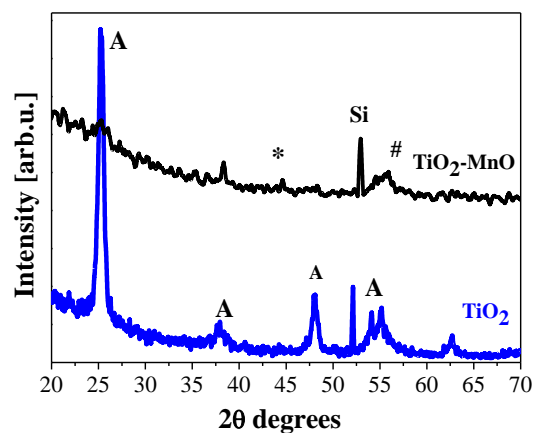


Figure 1. XRD patterns of TiO₂ and TiO₂-MnO films treated at 500 °C. The two symbols (* and #) denote Mn oxide fractions, A indicates anatase titania.

atmospheric CO₂ [16]. The absorption bands below 1000 cm⁻¹ are mainly due to metal-oxygen bonds. Figure 2 presents FTIR spectra of TiO₂ and TiO₂-MnO films annealed at 500 °C. The line at 668 cm⁻¹ seen in all spectra was associated with the Ti-O-Ti bridges of anatase [17]. The TiO₂ films exhibited weak bands at 590 cm⁻¹ and 462 cm⁻¹ related to the lattice vibration of anatase [17] and to the stretching mode of Ti-O bonds, respectively.

The main absorption band was split in two IR lines at 419 cm⁻¹ and 438 cm⁻¹ related to anatase phase, with the line at 438 cm⁻¹ known to be related with the fundamental Ti-O stretching mode of anatase [18]. The TiO₂ films annealed at 500 °C showed stronger IR lines attributed to anatase phase. The TiO₂-MnO films had different FTIR spectra, with the stronger bands at 440 cm⁻¹ and 420 cm⁻¹ matching those of single TiO₂ films proving anatase phase. The weak line at 502 cm⁻¹ seen after treatment at 500 °C was attributed to rutile TiO₂ [19]. The weak lines at 740 cm⁻¹, 670 cm⁻¹ and at 460 cm⁻¹ were connected with anatase phase [20]. The FTIR spectra of TiO₂-MnO films revealed other weaker but clearly observed absorption peaks at 606 cm⁻¹ (broad), 567 cm⁻¹ (shoulder) and 486 cm⁻¹ (weak for the 300 °C annealed film, but broader and well-defined for the 500 °C annealed sample). They were related to the O-Mn-O stretching mode [21], the Mn-O-Mn vibrations of manganese oxides [22] and the Mn-O bonds in Mn₂O₃ [6], respectively. The line at 547 cm⁻¹ was assigned to the stretching Mn-O-Ti vibrations [23]. The FTIR analysis confirmed the conclusions from the XRD study proving the formation of manganese phases together with anatase titania.

The film thickness of TiO₂ and TiO₂-MnO films is given in table 1. The thickness difference affects the film transparency.

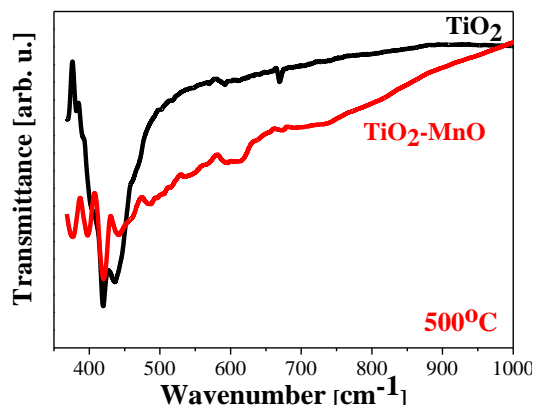


Figure 2. FTIR spectra of the sol-gel TiO₂ and TiO₂-MnO films annealed at 500 °C.

Table 1. Film thickness and estimated direct and indirect optical band gaps of the sol-gel films.

T _{annealing} [°C]	TiO ₂			TiO ₂ -MnO		
	d [nm]	Direct E _g [eV]	Indirect E _g [eV]	d [nm]	Direct E _g [eV]	Indirect E _g [eV]
300	120	3,87	3,50	190	3,71	3,02
500	100	3,85	3,44	150	3,69	2,98

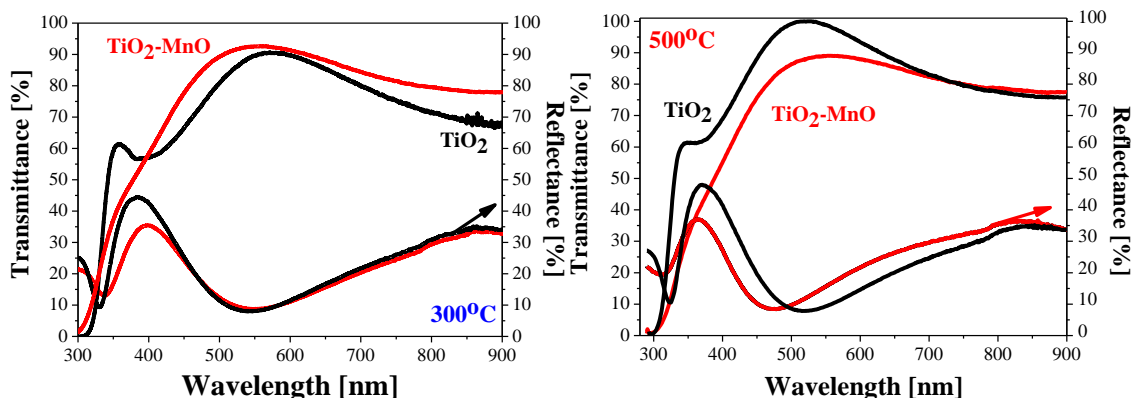


Figure 3. Transmittance and reflectance spectra of TiO₂ and TiO₂-MnO films deposited on glass substrates and annealed at 300 °C and 500 °C. The spectra are taken against a bare substrate.

Nevertheless, the thicker TiO₂-MnO film treated at the lower temperature manifested a better transmittance compared to single TiO₂ (figure 3). After annealing at 500 °C, the TiO₂ film had a higher transmittance. The TiO₂ films improved their transparency as the annealing temperatures was raised due to the higher crystallization degree and better stoichiometry. On the other hand, the TiO₂-MnO film transparency was reduced by the thermal treatment resulting in a more disordered structure (mixture of amorphous and crystal phases) and, probably, a rougher surface. The same effect could be seen for the TiO₂-MnO films deposited on conductive glass substrates (see figure 4).

The optical band gap was quantified by using the Tauc relation and the absorption coefficient was estimated from the spectrophotometric data. In this work, the indirect and direct band gaps was determined by extrapolating the linear portion of the plots $(\alpha h\nu)^{1/2}$ vs. $h\nu$ and $(\alpha h\nu)^2$ vs. $h\nu$ to the energy axis. The values obtained for the films deposited on glass are given in table 1. The TiO₂ semiconductor is reported to have direct and indirect band gaps [24]. The indirect optical band gap values for TiO₂ and TiO₂-MnO films are smaller than the corresponding direct band gaps. The direct and indirect E_g of the films studied in this work showed a slight narrowing as the annealing temperature was raised. This could be associated with structural transformations, a better crystallinity and greater crystallite sizes [25]. The XRD analysis revealed that the annealing at 500 °C resulted in TiO₂ films fully crystallized in anatase phase; while the TiO₂-MnO manifested crystallization in a mixture of Ti- and Mn-containing oxide crystal phases. Incorporating Mn in the TiO₂ matrix induced a significant narrowing of the optical band gap [26]. The reported E_g for MnOx are as follows: Mn₂O₃ from 2,50 – 2,86 eV [27, 28]. The optical band gap values determined of sol-gel TiO₂-MnO films are in good agreement with the reported values for mixed Ti-Mn oxide films deposited by different methods [29-31]. The optical characterization of TiO₂ and TiO₂-MnO films demonstrated that these materials are suitable for electrochromic applications; particularly good optical properties were exhibited by the TiO₂-MnO films annealed at the lower temperatures.

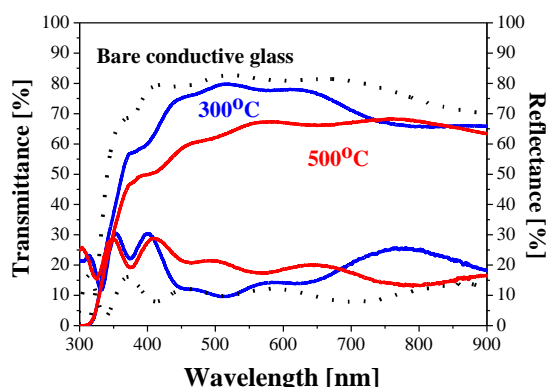


Figure 4. Transmittance and reflectance spectra of annealed TiO₂-MnO films deposited on conductive glass. The spectra of a bare substrate are given as reference.

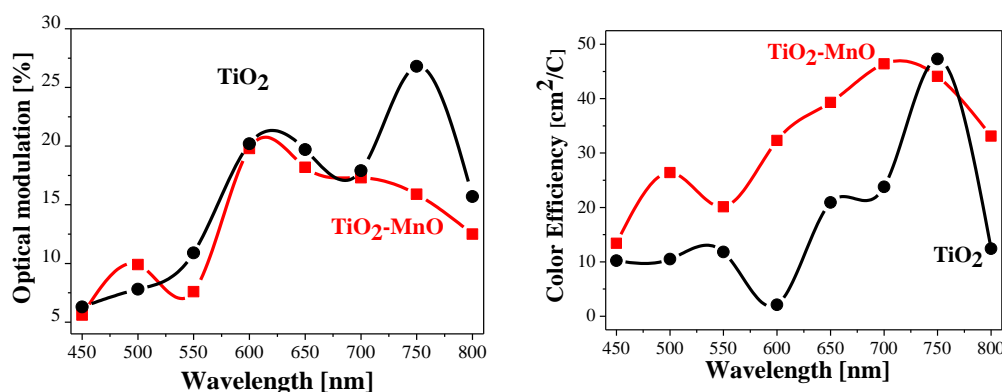


Figure 5. Optical modulation and color efficiency of TiO₂ and TiO₂-MnO films treated at 300 °C.

The electrochromic (EC) characterization was performed by cyclic voltammetric measurements at a scan rate of 20 mV/s. Upon Li^+ intercalation, the films were colored and their transmittance was low; when the Li^+ ions were extracted, the films were bleached (transparent state). The EC characteristics of the TiO_2 films significantly deteriorated with the annealing. The 500 °C-treated films possessed a color efficiency of up to 5 – 12 cm^2/C and optical modulation of 4 – 15 % in the wavelength range of 450 – 800 nm. The optical study demonstrated that the transmittance of the 500 °C TiO_2 -MnO films decreased rapidly. This is why, the EC properties were studied for films annealed at the lower temperature. The ΔT and CE values of the TiO_2 and TiO_2 -MnO films annealed at 300 °C are presented in figure 5. As seen, the optical modulation was a little lower than that of single TiO_2 , but the color efficiency values were higher. The study of the TiO_2 -based films showed that they are suitable for optoelectronic applications. The EC characteristics obtained are within the range of values reported earlier [32, 33].

4. Conclusions

Electrochromic films of TiO_2 and TiO_2 -MnO were successfully deposited by sol-gel dip-coating. The XRD study proved that the TiO_2 films crystallized in anatase phase. The TiO_2 -MnO films treated at 500 °C had a mixed structure of amorphous and crystal phases (anatase and Mn oxides). The FTIR spectroscopy also revealed the existence of Mn-O and Mn-Ti-O bonds. The optical study demonstrated a worsening of the TiO_2 -MnO film transparency with increasing the annealing temperature to 500 °C. A narrowing of the optical band gap of TiO_2 -MnO films was established. The color efficiency values of TiO_2 -MnO films were higher than those of the single titanium dioxide films and reached 46.4 cm^2/C (700 nm).

References

- [1] Surca A K, Dražić G and Mihelčič M 2019 *Sol. Energy Mater. Sol. Cells* **196** 185
- [2] Mjejri I, Gaudon M and Rougier A 2019 *Sol. Energy Mater. Sol. Cells* **198** 19
- [3] Xie S, Bia Z, Chen Y, Hea X, Guo X, Gao X and Li X 2018 *Appl. Surf. Sci.* **459** 774
- [4] Touam T, Znaidi L, Vrel D, Ninova-Kuznetsova I, Brinza O, Fischer A and Boudrioua A 2013 *Coatings* **3** 49
- [5] Şilik E, Pat S, Özen S, Mohammadigharehbagh R, Yudar H H, Musaoğlu C and Korkmaz Ş 2017 *Thin Solid Films* **640** 27
- [6] Isber S, Majdalani E, Tabbal M, Christidis T, Zahraman K and Nsouli B 2009 *Thin Solid Films* **517** 1592
- [7] Kernazhitsky L, Shymanovska V, Gavrilko T, Puchkovska G, Naumov V, Khalyavka T, Kshnyakin V, Chernyak V and Baran J 2010 *Mater. Sci. Eng. B* **175** 48
- [8] Naffouti W, Jrad A, Nasr T B, Ammar S and Turki-Kamoun N 2016 *J. Mater. Sci.: Mater. Electron.* **27** 4622
- [9] Harizanov O and Harizanova A 2000 *Sol. Energy Mater. Sol. Cells* **63** 185
- [10] Wen R T, Niklasson G A and Granqvist C G 2014 *Thin Solid Films* **565** 128
- [11] Wang H, Chen H, Wang Y and Lyu Y K 2019 *Chem. Eng. J.* **361** 1161
- [12] Harizanov O, Ivanova T and Harizanova A 2001 *Mater. Lett.* **49** 165
- [13] Wei L, Cui S, Guo H and Ma X 2018 *Mol. Catal.* **445** 102
- [14] León A, Reuquen P, Garín C, Segura R, Vargas P, Zapata P and Orihuela P A 2017 *Appl. Sci.* **7** 49
- [15] Praveen P, Viruthagiri G, Mugundan S and Shanmugam N 2014 *Spectroch. Acta A* **117** 622
- [16] Kaur G, Negi P, Kaur M, Sharma R, Konwar R J and Mahajan A 2018 *Ceram. Int.* **44** 18484
- [17] Ranjbar S, Saberyan K and Parsayan F 2018 *Mater. Chem. Phys.* **214** 337
- [18] Vuk A Š, Ješe R, Orel B and Dražić G 2005 *Int. J. Photoenergy* **07** 163
- [19] Busan T and Devine R A B 2005 *Semicond. Sci. Technol.* **420** 870
- [20] Adamczyk A and Dlugor E 2015 *Spectroch. Acta A* **145** 145
- [21] Jaganyi D, Altaf M and Wekesa I 2013 *Appl. Nanosci.* **3** 329
- [22] Sanchez-Botero L, Herrera A P and Hinstroza J P 2017 *Nanomater.* **7** 117

- [23] Enhessari M, Parviz A, Karamali E and Ozaee K 2012 *J. Exper. Nanosci.* **7** 327
- [24] Reddy K M, Manorama S V and Reddy A R 2003 *Mater. Chem. Phys.* **78** 239
- [25] Mathews N R, Morales E R, Cortés-Jacome M A and Antonio J A T 2009 *Sol. Energy* **83** 1499
- [26] Kernazhitsky L, Shymanovska V, Naumov V, Fedorenko L, Kshnyakin V, Shcherban N, Filonenko S and Baran J 2017 *J. Lumin.* **187** 521
- [27] Dubal D P, Dhawale D S, Salunkhe R R, Pawar S M, Fulari V J and Lokhande C D 2009 *J. Alloys Comp.* **484** 218
- [28] Belkhedkar M R and Ubale A U 2014 *J. Molec. Str.* **1068** 94
- [29] Mansoor M A, Mazhar M, Pandikumar A, Khaledi H, Ming H N and Arifin Z 2016 *Int. J. Hydrogen Energy* **41** 9267
- [30] Grace A A, Divya K P, Dharuman V and Hahn J H 2019 *Electroch. Acta* **302** 291
- [31] Brus V V, Pidkamin L J, Abashin S L, Kovalyuk Z D, Maryanchuk P D and Chugai O M 2012 *Optic. Mater.* **34** 1940
- [32] Khalifa Z S, Lin H and Shan S I 2010 *Thin Solid Films* **518** 5457
- [33] Dhandayuthapani T, Sivakumar R, Ilangovan R, Gopalakrishnan C, Sanjeeviraja C and Sivanantharaja A 2017 *Electrochim. Acta* **255** 358